Supplement of Atmos. Chem. Phys., 23, 12525–12543, 2023
https://doi.org/10.5194/acp-23-12525-2023-supplement

Atmospheric Chemistry and Physics
Open Access

Supplement of

Development and evaluation of processes affecting simulation of diel fine particulate matter variation in the GEOS-Chem model

Yanshun Li et al.

Correspondence to: Yanshun Li (yanshun.li@wustl.edu)

S1. The Federal Equivalent Method (FEM) in situ sites.

Fig. S1b shows the diel variation of the nine types of instruments used at FEM in-situ sites, which provide hourly measurements of $PM_{2.5}$ across the contiguous US. The number and location of instrument types are in Fig. 1. The majority (90.2%) of these instruments belongs to the first four types, which are shown in Fig. S1a. They exhibit generally consistent average diel profile of measured $PM_{2.5}$ mass, which we target as the typical variation to investigate. The other five types, shown as colored or dashed curves in Fig. S1b, deviated from the typical profiles. Specifically, the Teledyne Model 602 reports $PM_{2.5}$ concentrations variability which largely deviates from the typical pattern in Fig. S1a. The GRIMM Model 180 reports a pronounced morning peak. The Met One BAM-1022 exhibits a morning minimum of $PM_{2.5}$. The TEOM 1400 reports notably lower concentrations from midnight to early morning. Considering that these five types of instruments with deviated $PM_{2.5}$ diel patterns only account for less than 10% in all types, we exclude them from our analysis. Our analysis focuses on investigating the typical diel cycles in Fig. S1a.

S2. Spatial distribution of $PM_{2.5}$ in GEOS-Chem simulations and in situ measurements

Fig. S2a maps the annual $PM_{2.5}$ concentrations over the contiguous US simulated by the GC_Base simulation with the FEM/FRM in-situ measurements overlaid. The observed $PM_{2.5}$ concentrations are elevated over large parts of the Eastern contiguous US and the west coast. Other regions, primarily the mountainous Midwest, have relatively lower $PM_{2.5}$ levels with annual average concentrations below 10 $\mu g/m^3$. Nevertheless, local hotpots can still be identified for major cities (Denver, Salt Lake City, Phoenix) and national forests vulnerable to open fires (Nez Perce-Clearwater near the state boundary of Idaho/Montana, Okanogan-Wenatchee in north WA). The GC_Base simulation broadly captures the observed spatial variation of annual mean $PM_{2.5}$ over the contiguous US in 2016 with the Root Mean Square Deviations (RMSD) against the FRM/FEM in-situ measurements of 3.35/3.75 $\mu g/m^3$. The statistics for the FEM and FRM sites are consistent, providing a measure of confidence in the data quality of the hourly FEM measurements. The simulated concentrations are systematically biased high against observations by 28%. The contributors to this bias are peripherally explored but are not the main focus of this work. Fig. S2b maps the annual concentrations by the GC_2m_PBLH_NIT simulation, in which temporal resolution of emissions is increased from monthly to hourly, dry deposition scheme is updated, boundary layer height is adjusted, the vertical representativeness differences between model and observations are resolved and nitrate is constrained. The RMSD of the GC_2m_PBLH_NIT $PM_{2.5}$ against the FEM/FRM measurements drops from 3.35/3.75 to 2.74/2.84 $\mu g/m^3$. The overestimation of $PM_{2.5}$ in Eastern contiguous US and the west coast is reduced. These results indicate that our model updates improve on the simulation of annual mean concentrations.

S3. Design of supplementary simulations for investigating chemical pathways of nighttime $PM_{2.5}$ nitrate formation in GEOS-Chem

Following Travis et al., (2022), four additional sensitivity simulations (Table S3) were conducted based on GC_2m (Table 1) for identifying primary chemical pathways of nighttime $PM_{2.5}$ nitrate in GEOS-Chem. As shown in Table S3, GC_Chem_S1 turns off NO_2 hydrolysis (reaction R1), GC_Chem_S2 turns off N_2O_5 hydrolysis (reaction R2&R3), GC_Chem_S3 turns off NO_3 hydrolysis (reaction R4), and GC_Chem_S4 turns off all nighttime nitrate chemistry in GEOS-Chem (reaction R1-R4). In reaction R2, $\emptyset$=1 for sea salt aerosol and $\emptyset$=0 for all other aerosol types (Travis at al., 2022).

$$NO_2 \xrightarrow{aerosol} 0.5HNO_3 + 0.5HNO_2 \tag{R1}$$

$$N_2O_5 \xrightarrow{aerosol} (2-\emptyset)HNO_3 + \emptyset ClNO_2 \tag{R2}$$

$$N_2O_5 \xrightarrow{cloud} 2HNO_3 \tag{R3}$$

$$NO_3 \xrightarrow{aerosol/cloud} HNO_3 \tag{R4}$$

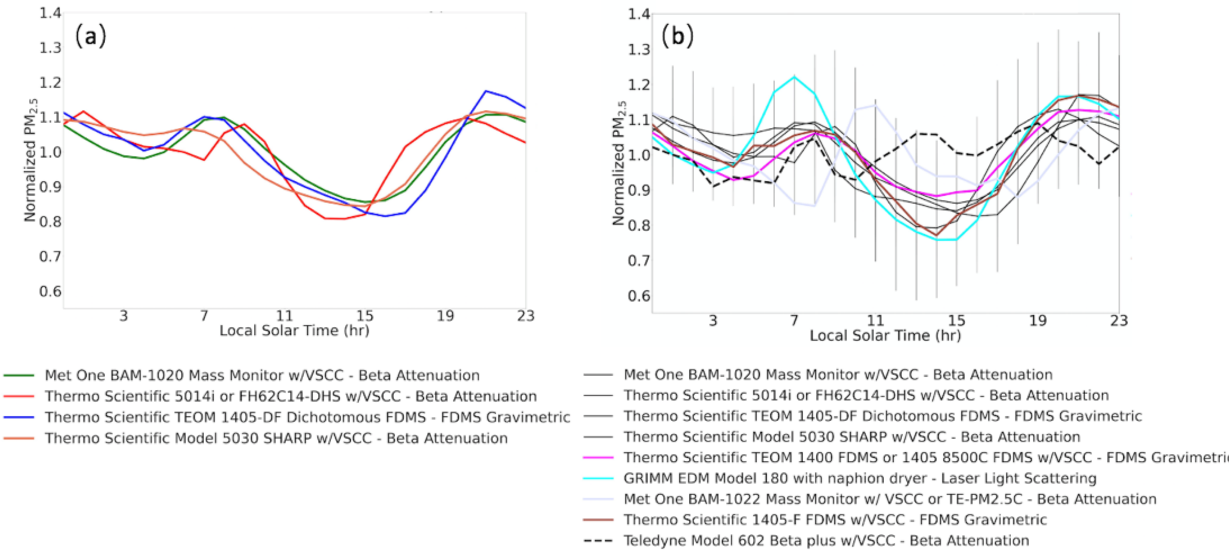

Figure S1. Average diel $PM_{2.5}$ variation of different FEM in-situ instruments over the contiguous US in 2016. (a) The major four types of instruments with typical diel $PM_{2.5}$ cycles. (b) All types of instruments.

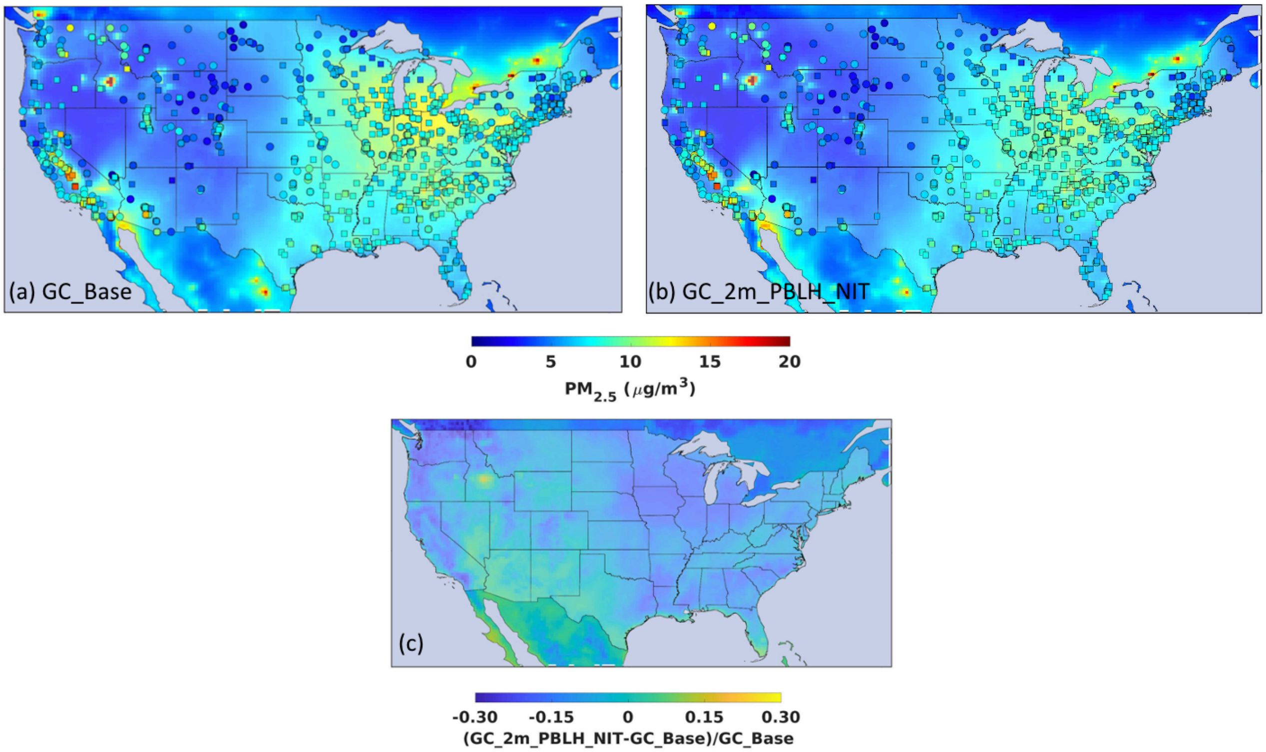

Figure S2. Annual $PM_{2.5}$ concentrations over the contiguous US in 2016. The background maps show modeled annual $PM_{2.5}$ concentrations by (a) the GC_Base simulation and (b) the GC_2m_PBLH_NIT simulation. (c) The difference between GC_Base and GC_2m_PBLH_NIT, calculated as (GC_2m_PBLH_NIT – GC_Base) / GC_Base. Overlaid filled circles represent in-situ FEM measurements. Filled squares represent in-situ FRM measurements.

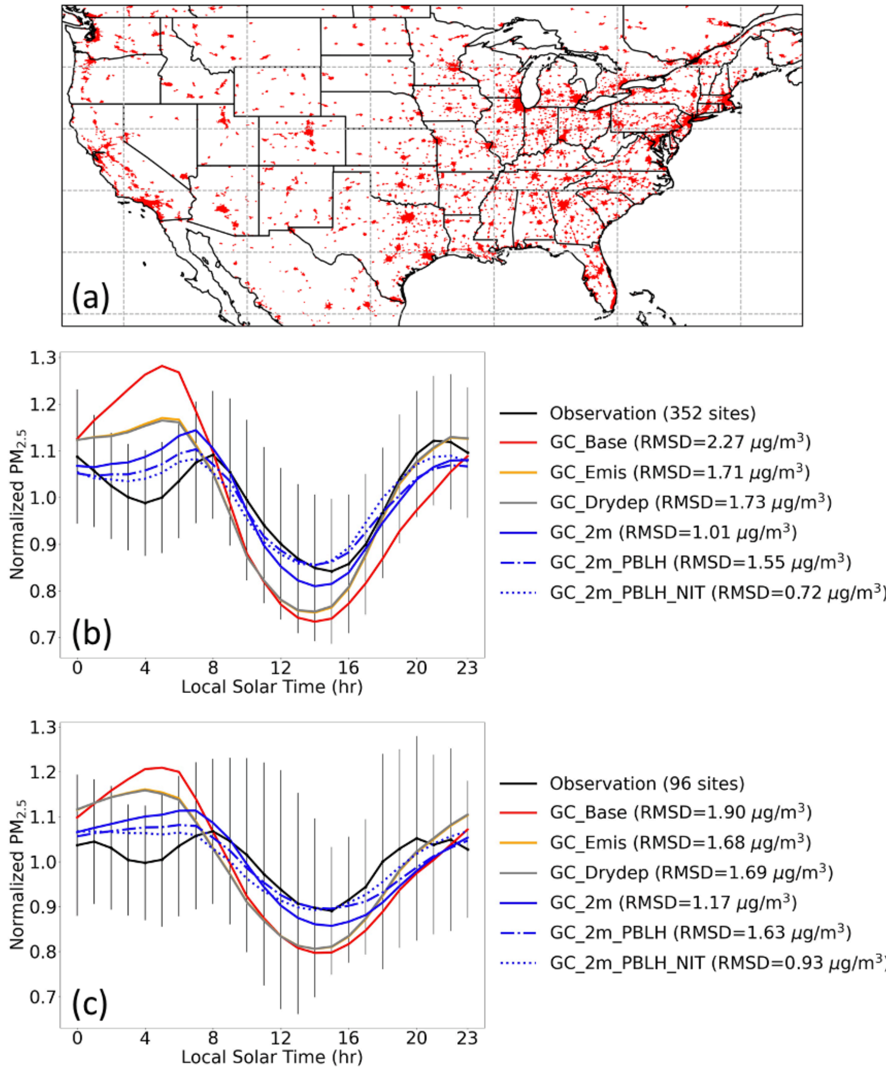

Figure S3. (a) Urban extent from the GRUMP v1 data. (b) Diel $PM_{2.5}$ over urban areas in the contiguous US. (c) Diel $PM_{2.5}$ over rural areas in the contiguous US.

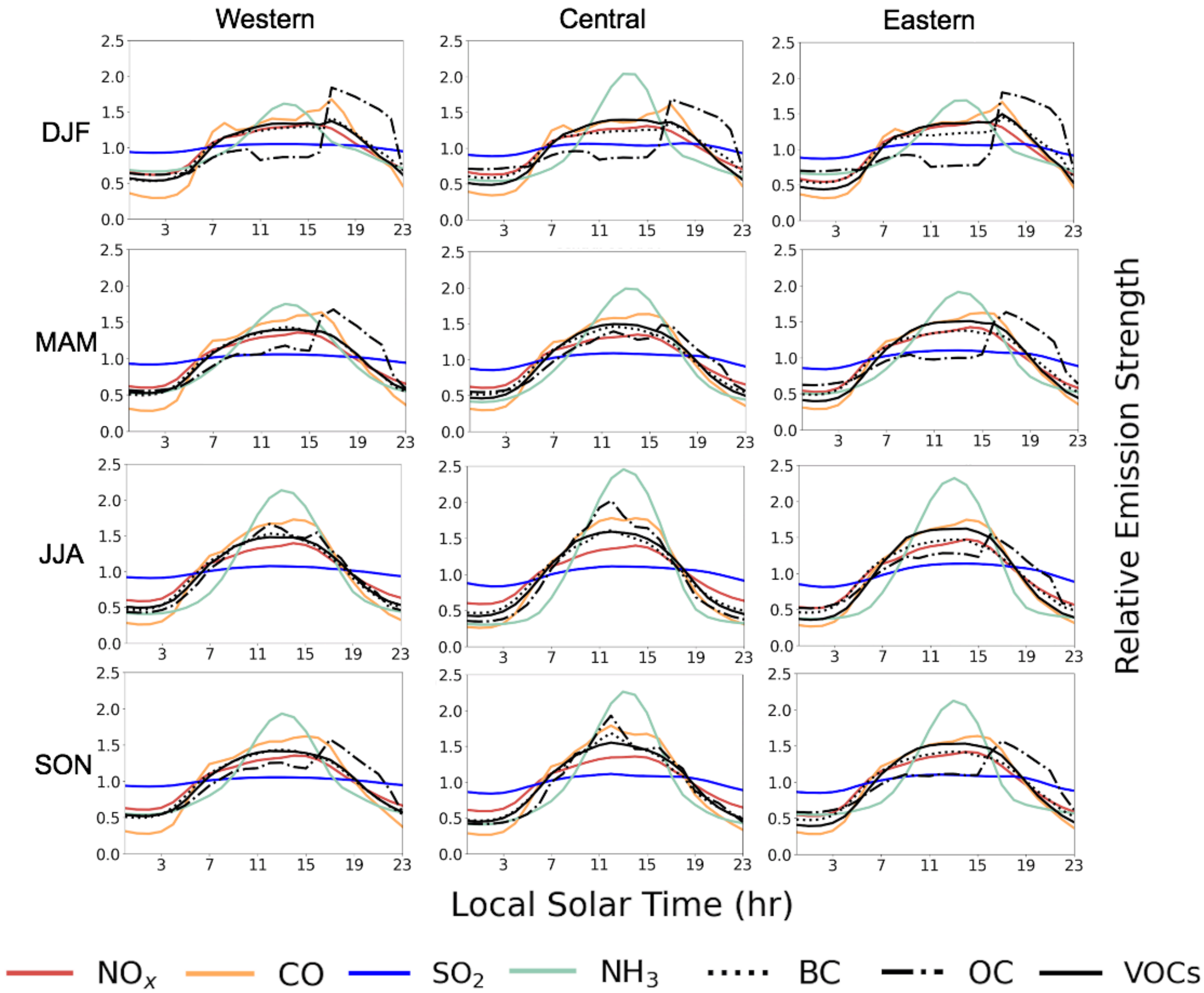

Figure S4. Normalized mean seasonal and regional diel profiles of speciated emissions from the EPA National Emission Inventory (NEI).

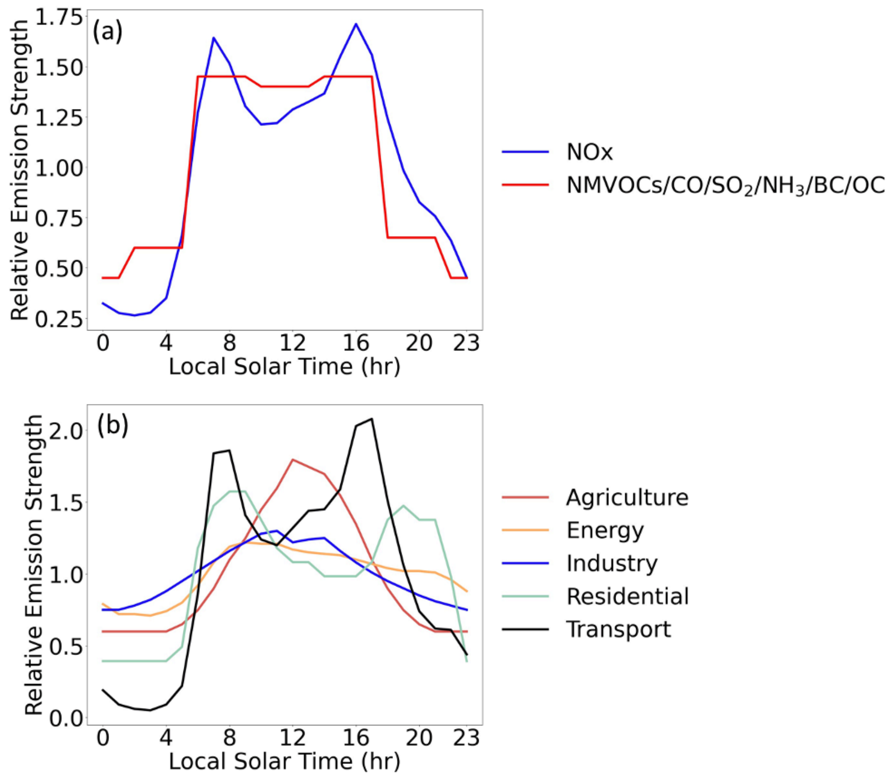

Figure S5. (a) Default species-specific diel scaling factors used in emission module of GEOS-Chem v12.6.0. (b) Sectoral diel scaling factors proposed in GEOS-Chem 14 (https://github.com/geoschem/geos-chem/issues/1824).

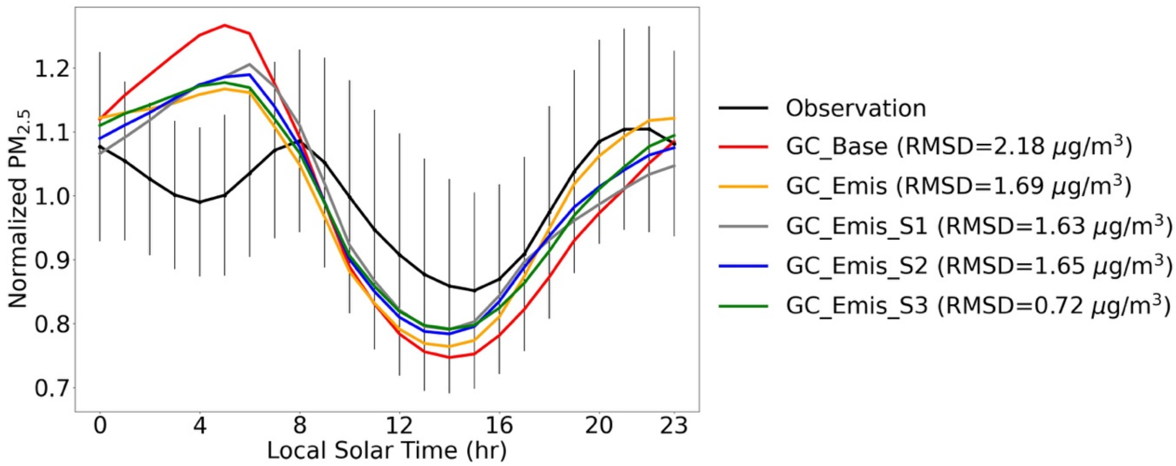

Figure S6. Diel $PM_{2.5}$ in sensitivity simulations in Table S2, GC_Emis, GC_Base and the FEM measurements.

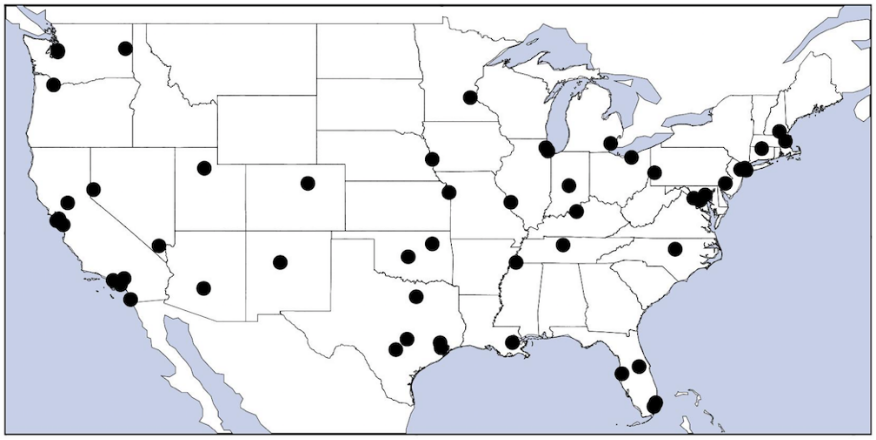

Figure S7. The Aircraft Meteorological Data Reports (AMDAR) sites.

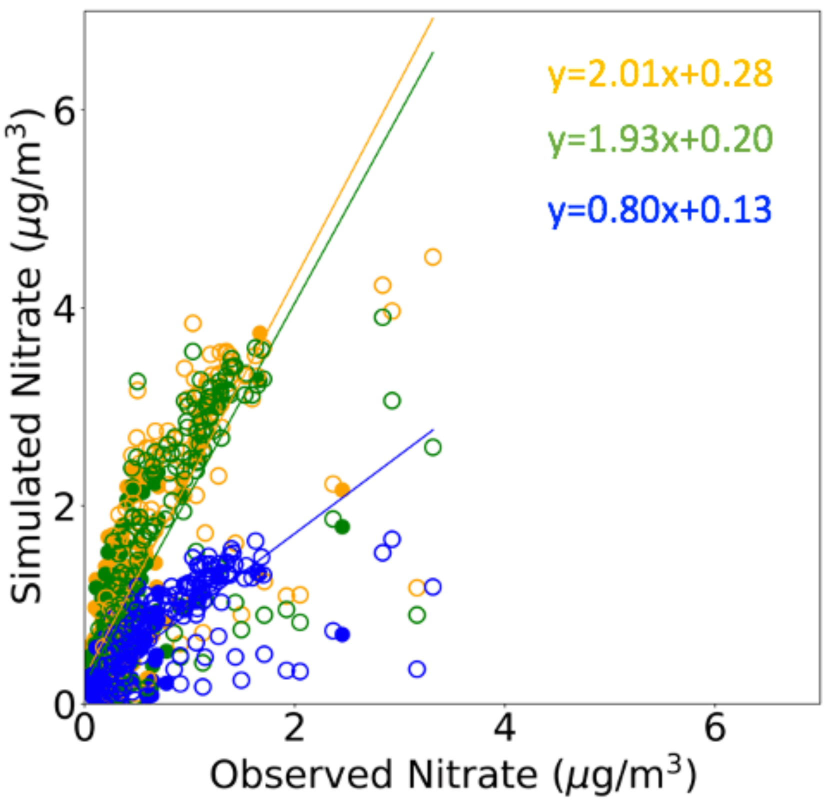

Figure S8. Mass concentrations of nitrate $PM_{2.5}$ in the GC_Base (orange), GC_2m_PBLH (green) and GC_Chem_S2 simulations (Table 1 & S3) in 2016. The filled/hollow circles represent in situ observations from the IMPROVE/CSN network (Solomon et al., 2014) respectively. Solid lines indicate lines of best fit determined with reduced major axis linear regression.

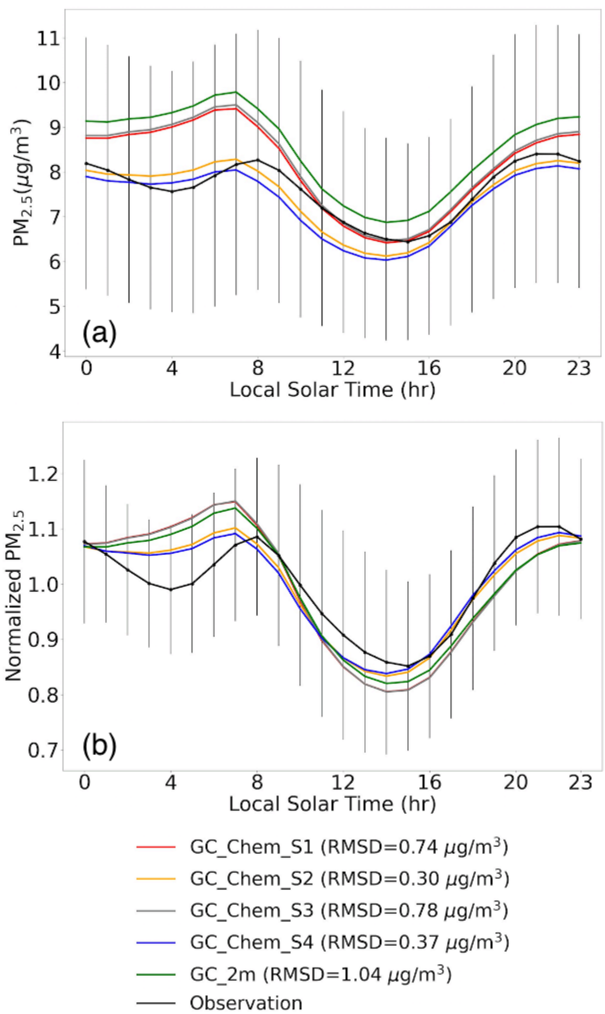

Figure S9. Diel profiles of $PM_{2.5}$ in the sensitivity simulations investigating nitrate chemical pathways during the night (Table S3). (a) $PM_{2.5}$ concentrations. (b) Normalized $PM_{2.5}$. Vertical lines represent spatial standard deviation of the measurements.

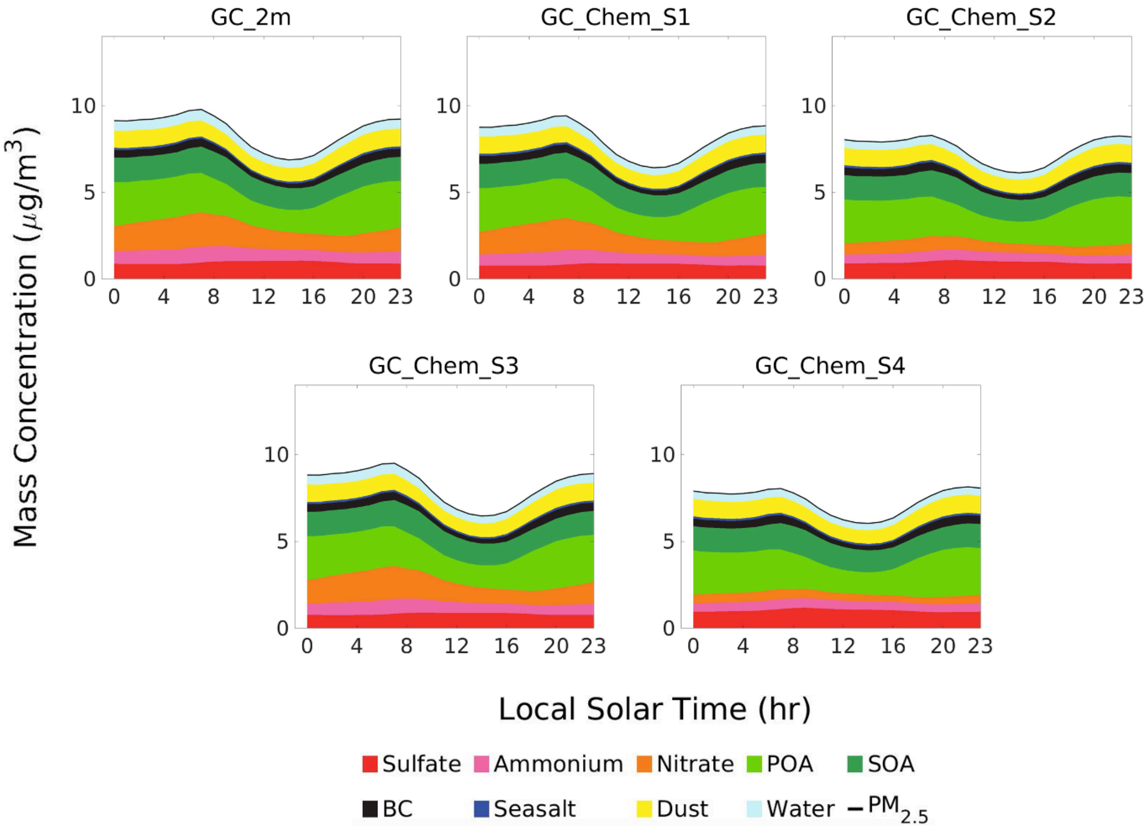

Figure S10. Diel profiles of $PM_{2.5}$ composition in the sensitivity simulations investigating nitrate chemical pathways during the night (Table S3).

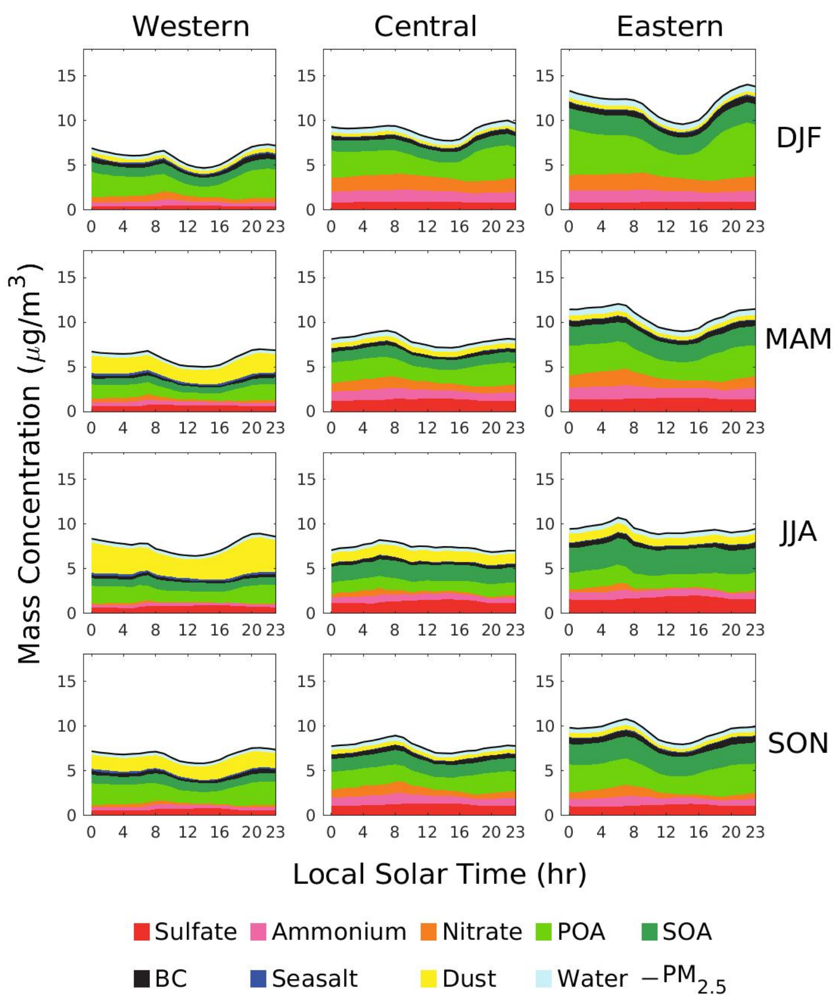

Figure S11. Seasonal and regional diel profiles of $PM_{2.5}$ composition in the GC_2m_PBLH_NIT (Table 1) simulation.

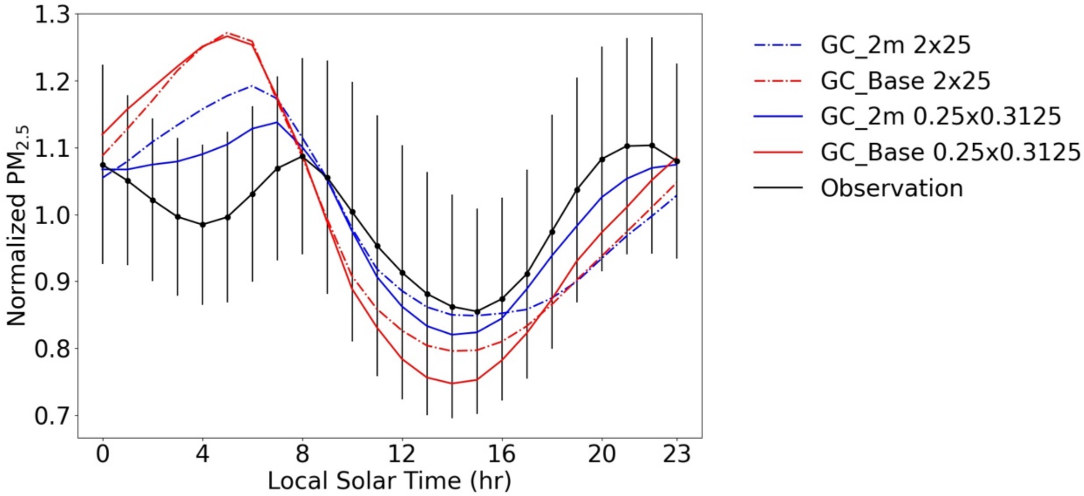

Figure S12. Diel $PM_{2.5}$ of the GC_Base and GC_2m simulations at different spatial resolution.

Table S1. RMSD of GEOS-Chem $PM_{2.5}$ against the FEM measurements. (Unit: $\mu g/m^3$)

Region	Season	GC_Base	GC_Emis	GC_Drydep	GC_2m	GC_2m_PBLH	GC_2m_PBLH_NIT
Western	DJF	2.38	2.13	2.11	3.04	2.79	3.45
	MAM	1.76	1.36	1.28	0.61	0.61	0.45
	JJA	1.66	1.36	1.31	1.07	0.90	0.88
	SON	1.37	0.98	0.96	0.95	0.44	0.67
Central	DJF	3.37	3.24	3.21	2.65	3.10	1.40
	MAM	2.80	2.49	2.43	1.98	2.46	1.41
	JJA	1.83	1.19	1.06	0.78	1.20	0.84
	SON	2.32	1.73	1.64	1.30	1.86	1.01
Eastern	DJF	4.77	4.71	5.01	4.37	4.87	3.10
	MAM	4.64	3.98	4.27	3.56	4.24	2.82
	JJA	2.79	1.79	1.92	1.36	2.16	1.76
	SON	3.10	2.39	2.55	1.83	2.52	1.67

Table S2. Supplementary GEOS-Chem simulations built upon GC_Emis (Table 1) to investigate impacts of emissions on diel $PM_{2.5}$ variation. GC_Emis_S1 uses monthly NEI emissions with the built-in diel scaling factors in GEOS-Chem v12.6.0 (Fig. S5a). GC_Emis_S2 uses monthly NEI emissions with the averaged scaling profiles shown in Fig. 4. GC_Emis_S3 uses monthly CEDS emissions with sectoral diel scaling factors (Fig. S5b) proposed for GEOS-Chem v14 (https://github.com/geoschem/geos-chem/issues/1824).

GEOS-Chem simulation	Base inventory	Temporal resolution of emissions	Diel Scaling Factors	Vertical representativeness	Aerosol dry deposition	Boundary layer mixing	Nitrate constrained
GC_Emis_S1	NEI	monthly	HEMCO	Lowest model level center	Default	Default	No
GC_Emis_S2	NEI	monthly	NEI species	Lowest model level center	Default	Default	No
GC_Emis_S3	CEDS	monthly	Sectoral average	Lowest model level center	Default	Default	No

Table S3. Supplementary GEOS-Chem simulations built upon GC_2m (Table 1) to investigate chemical pathways of $PM_{2.5}$ nitrate formation during the night.

GEOS-Chem simulation	Nitrate nighttime chemistry	Temporal resolution of emissions	Vertical representativeness	Aerosol dry deposition	Boundary layer mixing	Nitrate constrained
GC_Chem_S1	NO_2 hydrolysis (Reaction R1) turned off	NEI hourly	2m	Revised	Default	No
GC_Chem_S2	N_2O_5 hydrolysis (Reaction R2&R3) turned off	NEI hourly	2m	Revised	Default	No
GC_Chem_S3	NO_3 hydrolysis (Reaction R4) turned off	NEI hourly	2m	Revised	Default	No
GC_Chem_S4	All nighttime nitrate pathways (Reaction R1-R4) turned off	NEI hourly	2m	Revised	Default	No

References

Solomon, P. A., Crumpler, D., Flanagan, J. B., Jayanty, R. K. M., Rickman, E. E., and McDade, C. E.: U.S. National $PM_{2.5}$ Chemical Speciation Monitoring Networks—CSN and IMPROVE: Description of networks, Journal of the Air & Waste Management Association, 64, 1410–1438, https://doi.org/10.1080/10962247.2014.956904, 2014.

Travis, K. R., Crawford, J. H., Chen, G., Jordan, C. E., Nault, B. A., Kim, H., Jimenez, J. L., Campuzano-Jost, P., Dibb, J. E., Woo, J.-H., Kim, Y., Zhai, S., Wang, X., McDuffie, E. E., Luo, G., Yu, F., Kim, S., Simpson, I. J., Blake, D. R., Chang, L., and Kim, M. J.: Limitations in representation of physical processes prevent successful simulation of $PM_{2.5}$ during KORUS-AQ, Atmos. Chem. Phys., 22, 7933–7958, https://doi.org/10.5194/acp-22-7933-2022, 2022.